Appl Biochem Biotechnol (2008) 146:69–78
DOI 10.1007/s12010-007-8055-5

Cloning, Expression and Characterization of a Glycoside Hydrolase Family 39 Xylosidase from *Bacillus Halodurans* C-125

Kurt Wagschal · Diana Franqui-Espiet · Charles C. Lee · George H. Robertson · Dominic W. S. Wong

Received: 18 April 2007 / Accepted: 14 September 2007 /
Published online: 10 October 2007

Abstract The gene encoding a glycoside hydrolase family 39 xylosidase (*BH1068*) from the alkaliphile *Bacillus halodurans* strain C-125 was cloned with a C-terminal His-tag, and the recombinant gene product termed BH1068(His)$_6$ was expressed in *Escherichia coli*. Of the artificial substrates tested, BH1068(His)$_6$ hydrolyzed nitrophenyl derivatives of β-D-xylopyranose, α-L-arabinofuranose, and α-L-arabinopyranose. Deviation from Michaelis–Menten kinetics at higher substrate concentrations indicative of transglycosylation was observed, and k_{cat} and K_m values were measured at both low and high substrate concentrations to illuminate the relative propensities to proceed along this alternate reaction pathway. The pH maximum was 6.5, and under the conditions tested, maximal activity was at 47°C, and thermal instability occurred above 45°C. BH1068(His)$_6$ was inactive on arabinan, hydrolyzed xylooligosaccharides, and released only xylose from oat, wheat, rye, beech, and birch arabinoxylan, and thus, can be classified as a xylosidase with respect to natural substrate specificity. The enzyme was not inhibited by up to 200 mM xylose. The oligomerization state was tetrameric under the size-exclusion chromatography conditions employed.

Keywords Alkaliphile · Xylosidase · Glycoside hydrolase family 39 · Hemicellulose degradation

Introduction

Enzymes that can be harnessed for the breakdown of hemicellulose in cereal crops, and crop fiber biomass are becoming increasingly important because of their pivotal role in the utilization of these renewable energy sources. Hemicelluloses (xylans, arabinoxylans) are widely found as structural components in plant cell walls, where they cross-link with lignin and are extensively hydrogen-bonded to cellulose [1]. Structurally, xylans are heteropolysaccharides consisting of a linear β-D-(1→4)-linked xylopyranoside backbone that,

K. Wagschal (✉) · D. Franqui-Espiet · C. C. Lee · G. H. Robertson · D. W. S. Wong
USDA Agricultural Research Service, Western Regional Research Center,
800 Buchanan Street, Albany, CA 94710, USA
e-mail: kwagschal@pw.usda.gov

depending on the tissue source, is variously substituted with arabinose and other substituents. The xylose backbone of cereal xylans can be substituted with (1→2)- and/or (1→3)-linked α-L-arabinofuranosyl, α-D-glucuronic acid, and *O*-2 and/or *O*-3-linked acetate groups. Enzymes that hydrolyze non-reducing terminal β-D-xylopyranoside linkages and release xylose in an *exo*-manner from substrates such as xylooligosaccharides and arabinoxylan, and from synthetic substrates such as *p*-nitrophenyl-β-D-xylopyranoside are classified as xylan 1,4-β-xylosidases (xylosidases; EC 3.2.1.37). Xylosidases are key enzymes in the breakdown of biomass. Their action produces xylose from xylooligosaccharide mixtures that are produced by endo-xylanases. Moreover, because some xylanases can be inhibited by their xylooligosaccharide product, xylosidases can have a synergistic effect with endo-xylanase hydrolysis [2, 3]. Xylosidases and their potential biotechnological application have been the subject of several reviews [4–6]. In addition to the breakdown of hemicellulosic biomass for fuel and chemical feedstock use, xylosidases may also find use in cellulose pulp biobleaching processes [7].

Numerous enzymes with the ability to hydrolyze the various hemicellulose linkages have been isolated, most of them from microbial sources [6]. We describe in this paper the cloning with a C-terminal His-tag of the gene annotated *BH1068* from *Bacillus halodurans* C-125 genomic DNA, an alkalophilic bacterium with a known genomic sequence, and the subsequent expression, purification, and biochemical characterization of the encoded xylosidase gene product termed BH1068$(His)_6$.

Materials and Methods

Cloning BH1068 from Genomic DNA into pET 22 b(+)

Bacillus halodurans C-125 genomic DNA was obtained from the American Type Culture Collection (Manassas, VA, USA). The gene *BH1068* (1,509 bp, GenBank accession number BA000004) was amplified in a polymerase chain reaction using the following primers:

BH1068bl-5′: ATGAAAACAGTAGTTGTAAATGATCGTTC
BH1068–3′: GGATACTCGAGATACGAAGGAATCAGCCGA

The cloning strategy consisted of a 5′ blunt end and a 3′ *Xho*I cohesive terminal, and a pET-22b(+) vector was used for expressing the *BH1068* with a C-terminal His-tag. The amplified fragment was gel-purified using Promega SV gel and polymerase chain reaction (PCR) clean-up system (Promega, Madison, WI, USA). The product was digested with *Xho*I and subsequently purified using the Promega system. The expression vector used was pET22b(+) digested with *Nde*I *and Xho*I. The digested vector was gel purified using the Promega System. Given that *BH1068* contains an internal *Nde*I site, the enzyme T4 DNA polymerase (Promega) was used to fill the 5′ end of the digested pET22 b(+) vector and convert it into a blunt end. Fragment and vector were ligated using T4 DNA ligase (Promega). BL21-Gold (DE3) chemically competent cells (Stratagene) were transformed with the construct.

BH1068$(His)_6$ Expression and Purification

The expression host *Escherichia coli* BL21(DE3) was transformed with the expression plasmid pET22b(+) containing the BH1068$(His)_6$ insert, streaked onto Luria–Bertani agar plates amended with 50 μg/ml carbenicillin (Sigma; LB_{carb}), and incubated overnight at 37°C.

Positive transformants were selected based on enzymatic hydrolysis of *p*-NP-β-D-xylopyranoside (described below) and restriction digestion of the plasmids. A single positive transformant was used to inoculate a 15-ml seed culture of *E. coli*, which was then grown in LB_{carb} broth at 37°C at 250 rpm for 16 h with 0.5% glucose added to repress protein expression. A 5-ml aliquot was used to inoculate 200 ml LB_{carb}, which was grown at 37°C to $OD_{600\,nm}$=2–3. Then 1 mM isopropylthiogalactoside was added to induce protein expression, and incubation was allowed to proceed at 16°C at 250 rpm for 16 h. Fifty milliliter aliquots were pelletted and the pellets stored frozen at −80°C. Cell lysis and release of soluble proteins were achieved by adding to each pellet 3.5 ml Bug-Buster solution (EMD Biosciences) containing 40 U/ml r-lysozyme (EMD Biosciences), 0.5 mM phenylmethylsulfonylfluoride, 25 U/ml benzonase, and 5 mM β-mercaptoethanol (BME; all from Sigma). Cells were incubated in the lysis solution for 20 min at room temperature, cooled to 0–4°C, and centrifuged to remove cell debris. The protein was purified using Ni-NTA resin (Qiagen) according to the manufacturer's instructions by first adjusting the supernatant solution to 300 mM NaCl, 10 mM imidazole, and 50 mM phosphate buffer (pH 8.0). The composition of the wash buffer used was 50 mM phosphate buffer (pH 8.0) containing 1 mM BME, 1 μl/ml Calbiochem protease inhibitor cocktail set III (EMD Biosciences), 300 mM NaCl, and 10 mM imidazole. The protein was eluted using the same buffer, except that the imidazole concentration was increased to 250 mM. Fractions containing the enzyme were buffer exchanged using NAP-5 desalting columns (Amersham Biosciences, Piscataway, NJ, USA) into 50 mM phosphate (pH 6.0), 10% glycerol, and 1 ul/ml protease inhibitor cocktail set III, and stored at −80°C. Protein concentrations were determined using Coomassie Plus reagent (Pierce Biotechnology, Rockford, IL, USA) following the manufacturer's protocol. Enzyme fractions were analyzed using polyacrylamide gel electrophoresis (PAGE, 4–12%, reducing) following the manufacturer's protocol (Invitrogen). Final protein purity was estimated to be 55% by gel densitometry performed using an AlphaImager imaging system (Alpha Innotech Corp., San Leandro, CA, USA).

Molecular Weight Determination

The molecular weight of the His-tagged protein was estimated by gel filtration chromatography using an Amersham/Pharmacia HiPrep 16/60 Superdex 200 10/300 GL column (Amersham Biosciences). The running buffer was 50 mM phosphate (pH 7.4), 150 mM NaCl, and 1 mM dithiothreitol (DTT). A standard curve was generated with low-molecular weight (13.7 to 67 kDa) and high-molecular weight (158 to 669 kDa) standards (Amersham Biosciences).

Enzyme Assays

For assays using nitrophenyl (NP) glycosides as substrates (Sigma, St. Louis, MO, USA or Research Products International Corporation, Mt. Prospect, IL, USA), the enzyme activity was determined by measuring the change in absorbance at 400 nm caused by NP release using a SpectraMax M2 spectrophotometer equipped with a temperature controller (Molecular Devices, Sunnyvale, CA, USA). Time-course studies using saturating substrate concentrations were initially performed with *p*-NP-XylP to establish the linearity of hydrolysis rate with respect to time at 45°C. In a typical kinetic assay, 190 μl of 50 mM phosphate (pH 6.5) containing 0.1% bovine serum albumin (BSA; Sigma) and varying substrate concentrations was pre-incubated at 45°C for 5 min, then 10-μl enzyme solution was added and mixed to initiate the reaction. Generally, 16 different substrate

concentrations were used to assess the kinetic parameters; the assays were performed in quadruplicate, and the amount of enzyme was chosen so that the proportion of substrate hydrolyzed at the end of the data acquisition period was 10% or less (Table 1). The kinetic parameters V_{max} and K_m for the aryl-glycoside substrates were calculated by non-linear regression fitting of the data to the Michaelis–Menten equation using the program GraFit 5 (Erithacus Software, Surrey, UK). The inhibition constant K_i for xylose was determined using a kinetic spectrophotometric assay wherein velocity was measured in the absence of added xylose, and then in the presence of 30, 60, 90, 120, and finally, 200 mM xylose using *p*-NP-XylP concentrations ranging from 30 to 2,000 μM, 50 mM phosphate (pH 6.5) and 20 nM BH1068(His)$_6$. Xylose at the various concentrations and BH1068(His)$_6$ were preincubated in the assay buffer for 10 min at 45°C, and the reaction initiated by adding *p*-NP-XylP.

The hydrolysis of the natural substrate xylobiose (Wako Chemicals USA, Inc., Richmond, VA, USA) was assessed using 380 nM BH1068(His)$_6$ and substrate concentrations of 1,040 μM to 16 mM, 100 mM phosphate buffer (pH 6.5), and a 35-min incubation at 45°C (Table 1). Xylotriose (Wako Chemicals USA, Inc., Richmond, VA, USA) and xylotetraose (Megazyme Ltd., Wicklow, Ireland) were also tested as substrates at concentrations ranging from 112 to 4480 μM for the former, and 104 μM to 16 mM for the latter. Enzyme activity resulting in xylose release was then assessed using an enzyme-coupled assay for xylose as described [8].

Activity Versus pH Profile

The effect of pH on the apparent V_{max} (Fig. 1) was measured using endpoint assays utilizing an equal volume of 1 M Na_2CO_3 to quench the reactions and raise all the pH values to ~pH 11. Reactions were carried out at 45°C using 4 mM *p*-NP-XylP, 68 nM BH1068(His)$_6$, 0.1% BSA, and incubation for 40 min at 35°C, followed by quenching with an equal volume of 1 M Na_2CO_3 and absorbance measurement at 400 nm. The buffers used to generate the pH curve were 100 mM citrate for pH 3 to 6.5, 100 mM phosphate for

Table 1 Michaelis–Menten kinetic parameters for hydrolysis of *p*-NP-AraF, *p*-NP-AraP, *p*- and *o*-NP-XylP, and xylobiose.

Substrate[a]	Concentration range (μM)	*K*m (μM)	k_{cat} (s^{-1})	k_{cat}/*K*m (mM^{-1} s^{-1})
p-NP-AraF	16–160	140±59.4	0.0043±0.0011	0.031±0.015
	16–4267	6030±419	0.080±0.0039	0.013±0.001
p-NP-AraP	16–160	713±148	0.15±0.03	0.21±0.06
	16–4267	4540±440	0.82±0.05	0.18±0.02
p-NP-XylP	10–150	30.1±2.97	0.184±0.006	6.10±0.64
	10–4515	3270±907	1.73±0.286	0.53±0.17
o-NP-XylP	10–375	11.5±5.76	0.235±0.021	20.4±10.3
	10–4,000	262±98.0	0.518±0.059	1.98±0.77
Xylobiose	1,040–16,000	30,900±8,100	0.35±0.07	0.011±0.004

[a] BH1068 enzyme concentrations were 163 nM for both *p*-NP-AraF and *p*-NP-AraP, 19 nM for both *p*- and *o*-NP-XylP, and 380 nM for xylobiose. Reaction conditions were 100 mM PO_4, pH 6.5, 45°C with 0.1% BSA. Ten percent or less conversion for *p*-NP-XylP, 8% or less conversion for *o*-NP-XylP, 5% or less conversion for *p*-NP-AraF, 7% or less conversion for *p*-NP-AraP, 2% or less conversion for xylobiose.

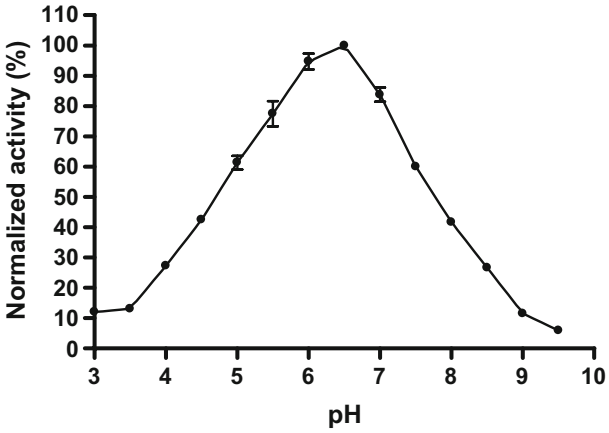

Fig. 1 Relative enzyme activity at the indicated pH values. Enzyme activity was determined with 4 mM *p*-NP-XylP (*circle*). Reaction conditions were as described in "Materials and Methods"

pH 6.5 to 8.0, and 100 mM AMPSO for pH 8.0 to 9.5. Reported values are the average of six determinations.

Thermostability Profiles and Temperature Versus V_{max}

The effect of temperature on enzyme stability (Fig. 2) was determined by first measuring the rate of *p*-NP-XylP hydrolysis before thermal challenge. The assays were performed in triplicate, and the reaction conditions were 45°C, 50 mM phosphate, pH 6.5, 0.1% BSA, 4 mM *p*-NP-XylP, and 19 nM BH1068(His)$_6$. Then 50-µl aliquots of the enzyme solution were transferred to a 96-well PCR plate and subjected to incubation at a series of temperatures ranging from 30 to 88.5°C for 10 min using a temperature gradient PCR machine (MJ Research, Watertown, MA, USA). After thermal treatment, the enzyme activity was again measured to allow calculation of the residual activity. The residual activity was then normalized to the highest recorded initial activity. The data shown in Fig. 2 are the average of either two or three measurements.

The effect of temperature on the apparent V_{max} was determined by performing endpoint assays using 64 nM BH1068(His)$_6$, 50 mM HPO_4 pH 6.5, 0.1% BSA, and 4 mM *p*-NP-

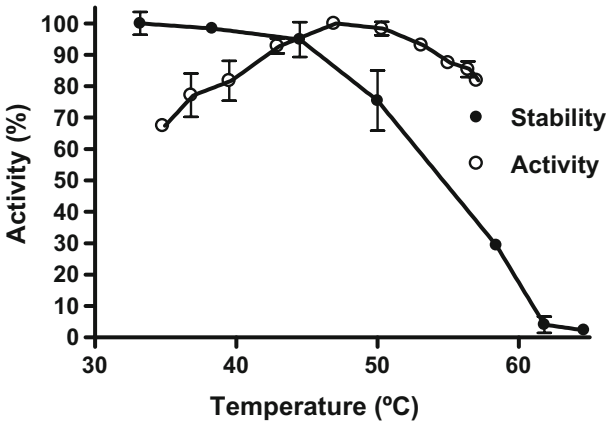

Fig. 2 Enzyme stability at the indicated temperatures (*filled circle*) and enzyme activity (relative V_{max}) at the indicated temperatures (*open circle*). Reaction conditions were as described in "Materials and Methods"

XylP. BH1068(His)$_6$ was incubated for 30 min at the various temperatures, quenched with an equal volume of Na_2CO_3, and *p*-NP release quantitated at 400 nm using a standard curve generated on the same microtiter plate. The data shown in Fig. 2 are the average of either three or four measurements.

Substrate Specificity

Capillary electrophoresis (CE) was used to monitor the degradation of the following natural polymeric substrates: sugar beet arabinan, rye flour arabinoxylan, wheat medium viscosity arabinoxylan (all from Megazyme), birchwood xylan, beechwood xylan, and oat spelt xylan (all from Sigma). The composition of these natural substrates were specified by the supplier as follows. The sugar beet arabinan substrate consisted of a 1,5-α-linked arabinose backbone to which 1,3-α-linked and possibly some 1,2-α-linked L-arabinofuranosyl groups were attached. Approximately 60% of the main-chain arabinofuranosyl residues were substituted by single 1,3-linked arabinofuranosyl groups. The cereal grain natural arabinoxylan substrates had homopolymeric backbones of (1–4)-β-D-xylopyranosyl residues substituted with (1–2)- and/or (1–3)-α-linked L-arabinofuranosyl branch units. The wheat arabinan medium viscosity arabinoxylan had an arabinose/xylose/other sugars ratio of 37:61:2. The rye flour arabinoxylan had a sugar composition of arabinose/xylose/other sugars of 49:48:3. The oat spelt xylan used contained minimally 70% xylose and maximally 10% arabinose and 15% glucose. The xylans from the two hardwoods, birchwood and beechwood, that were also tested were each specified as containing >90% xylose residues. Reaction conditions were overnight incubation at 37°C in 115-μl volume of reaction buffer containing 100 mM phosphate, pH 6.5, 1 μl/ml Calbiochem protease inhibitor cocktail III, 5 mM DTT, 0.1% BSA, and natural substrate concentrations between 0.9 and 2.2 mg/ml and 2.9 μM BH1068(His)$_6$. The samples were centrifuged, and a 100-μL aliquot from each reaction was lyophilized before derivatization. The reaction products formed using xylobiose as the substrate were also analyzed by CE, where the reaction conditions were 380 nM enzyme and 20 mM xylobiose, and reaction conditions were the same as those used for the other natural substrates. For the xylobiose reactions, 4 μl aliquots were removed at time 0 and, subsequently, at 30-min intervals, and the reaction quenched by heating to 100°C. 1-Aminopyrene-3,6,8-trisulphonate (APTS) derivatization was performed by adding 6 μl 100 mM APTS in 15% acetic acid and 12 μl 1 M $NaBH_3CN$ in tetrahydrofuran (THF) and allowing the derivatization reaction to occur overnight at 37°C. The samples were then stored at −20°C, and aliquots were diluted 200 to 400-fold before capillary electrophoresis. Analyses were performed on a P/ACE MDQ capillary electrophoresis system (CE, Beckman Coulter, Inc., Fullerton, CA, USA). Separations were performed using a 20-cm uncoated fused-silica capillary column of 50 μm internal diameter (MicroSolv Technology Corp., Long Branch, NJ, USA). Analyses were carried out at 25°C with an applied voltage of 30 kV using 50 mM phosphate, pH 7.4, as the running electrolyte. A typical run schedule was 0.5 min at 50 psi 0.1 N HCl, 0.5 min at 50 psi H_2O, 0.5 min at 50 psi 0.1 N NaOH, 0.5 min at 50 psi 1 M phosphate at pH 7.4, 4 min at 80 psi 50 mM phosphate at pH 7.4, conditioning at 30 kV for 5 min, injection 5 s at 0.5 psi, and separation at 30 kV. The detection system was a Beckman laser-induced fluorescence detector using an excitation wavelength of 488 nm and detection at 520 nm.

Action on the following artificial aryl-glycoside substrates was tested: *p*-NP-β-D-xylopyranoside (*p*-NP-XylP), *o*-NP-β-D-xylopyranoside (*o*-NP-XylP), *p*-NP-α-L-arabinofuranoside (*p*-NP-AraF), *p*-NP-α-L-arabinopyranoside (*p*-NP-AraP), *p*-NP-β-D-glucopyranoside, *p*-NP-β-D-fucopyranoside, *p*-NP-β-D-galactopyranoside, and *p*-NP-β-D-mannopyranoside (all from Sigma or Research Products International Corporation). Reaction conditions were

37 nM BH1068(His)$_6$, 4 mM aryl-glycoside substrate, 100 mM phosphate buffer at pH 6.5, 0.1% BSA, and 45°C. NP group release was monitored by measuring the change in absorbance at 400 nm.

Results and Discussion

Sequence Analysis

The xylosidases from several bacterial species have been characterized and, based on amino acid sequence similarity, have been classified into glycoside hydrolase (GH) families 3, 39, 43, 52, and 54 in the CAZy classification (P. M. Coutinho and B. Henrissat, http://www.afmb.cnrs-mrs.fr/CAZY) [9]. Phylogenetic analysis of the evolutionary relationship of the amino acid sequence of *BH1068* revealed greatest similarity to GH 39 proteins from *Geobacillus stearothermophilus* T-6 (UniProt Q9ZFM2; 65% identity, 76% consensus), *Thermoanaerobacterium saccharolyticum* (UniProt P36906; 62% identity, 72% consensus), and *Clostridium cellulolyticum* H10 (NCBI protein id ZP_01574178; 61% identity, 73% consensus). These enzymes are all members of the GH family 39 and are predicted to have xylosidase activity. Thus, based on amino acid sequence, BH1068(His)$_6$ belongs to GH family 39; this family has both β-D-xylosidase (EC 3.2.1.37) and α-L-iduronidase (EC 3.2.1.76) as known activities.

Alignment of the amino acid sequences of BH1068(His)$_6$ with xylosidases whose active site residues are known [10, 11] shows high homology around the active-site residues, with Glu160 predicted to be the acid/base catalyst and Glu279 predicted to be the nucleophile (*vide infra*).

Oligomerization State

The protein BH1068(His)$_6$ eluted as a single peak during gel filtration chromatography with an apparent MW value of ~235 kDa. Thus, the protein eluted as a tetramer under the conditions employed since the calculated subunit MW is 59.3 kDa based on the amino acid sequence predicted for the His-tagged protein. This is in contrast to the results of another study of BH1068(His)$_6$ wherein the data did not allow differentiation between dimeric and trimeric states for the C-terminal His-tagged enzyme [12]. However, the closely related β-xylosidases from *T. saccharolyticum* (62% identity, 72% consensus) and from *Geobacillus stearothermophilus* T-6 (65% identity, 76% consensus) have both been crystallized, and their quaternary structures shown to be tetrameric [10, 11].

Enzyme Kinetic Parameters

The catalytic mechanism of hydrolysis is conserved for all members within a given sequence-based GH family [13, 14] and has been reported to result in retention of the anomeric center in GH family 39 glycohydrolases. In the case of retaining hydrolytic enzymes, a double-displacement reaction ensues [15], and for GH, a pair of carboxyl groups are a central feature of the catalytic site. For retaining GH, one active-site carboxylate acts as a nucleophile where it attacks the sugar anomeric center to form an enzyme-bound covalent intermediate (xylosylation, k_2), whereas the other carboxylate groups acts as a general acid/base catalyst where it protonates the glycosidic oxygen concomitantly with bond cleavage in the first step (general acid catalysis) and deprotonates water in the second step (general base catalysis), resulting in formation of a β-sugar hemiacetal product (dexylosylation, k_3; Eq. 1)

[16–18]. Alternatively, another substrate molecule or other nucleophile can react with the covalent intermediate E–X in a transglycosylation reaction (k_4). This can lead to non-Michaelis–Menten kinetics when the apparent V_{max} continues to increase with increasing substrate concentration caused by an increase in k_4.

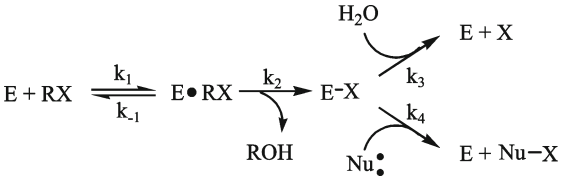

(1)

Time-course studies initially performed established that the rate of *p*-NP-XylP substrate hydrolysis under saturating conditions was linear with respect to time (R^2>0.99) for at least 35 min at 45°C. The Michaelis–Menten parameters for hydrolysis of *p*-NP-AraF, *p*-NP-AraP, *o*- and *p*-NP-XylP and xylobiose are shown in Table 1. For all of the substrates tested, deviation from Michaelis–Menten kinetics with increasing substrate concentration was observed, suggesting the participation of transglycosylation in the kinetic scheme. Transglycosylation has previously been observed for a related GH 39 xylosidase from *T. saccharolyticum* with the substrate xylobiose [8, 19] and also with aryl glycosides [8, 17]. *p*-NP-AraF was a very poor substrate, and the kinetic parameters obtained were not precise at low substrate concentrations because of an extremely low k_{cat}. Nevertheless, it can be concluded that while the K_m values for *p*-NP-AraF and *p*-NP-AraP were in the same range at both the low and high substrate concentrations tested, the k_{cat} values for the arabinopyranose aryl glycoside were roughly an order of magnitude greater than the corresponding values for the arabinofuranose congener, with the net result being the specificity factor k_{cat}/K_m was about tenfold larger for *p*-NP-AraP. The K_m for *o*-NP-XylP was in the low micromolar range, and a precise value was not obtained because the lowest substrate concentration tested was on the order of the K_m value for the substrate. However, the xylopyranoside substrates are clearly preferred over the arabinopyranoside substrates, with a 30-fold higher k_{cat}/K_m value at low substrate concentration ranges for *p*-NP-XylP than for the corresponding C4 epimer *p*-NP-AraP. It was interesting to note that the enzyme showed a lesser propensity for transglycosylation with *o*-NP-XylP compared to the *p*-NP analog, where k_{cat} at higher substrate concentrations only doubled for the *o*-NP isomer, compared to a tenfold difference for the *p*-NP isomer. Contributing significantly to the observed differences in hydrolysis rates and propensities for transglycosylation of *o*- and *p*-NP-XylP are differences in the noncovalent enzyme/substrate interactions (e.g., hydrogen bonding) of these stereoelectronically different leaving groups in the active site and the attendant differences in stabilization of their respective oxocarbenium ion-like transition states [16]. Thus, results similar to BH1068(His)$_6$ have previously been reported for a GH family 52 β-xylosidase, where k_{cat} *o*-NP-XylP/k_{cat} *p*-NP-XylP was ~4, whereas K_m values were similar [20]. On the other hand, similar k_{cat} values for *o*- and *p*-NP-XylP hydrolysis have been reported for a phylogenetically closely related GH family 39 β-xylosidase [21].

When xylobiose was tested as a substrate, deviation from Michaelis–Menten kinetics consistent with transglycosylation activity was observed at higher substrate concentrations (up to 16 mM xylobiose was tested). Capillary electrophoresis analysis of the reaction products from xylobiose hydrolysis showed production of significant xylose and xylotriose, corroborating the transglycosylation activity inferred by the kinetic data. Thus, under the

reaction conditions described, after 30 min, roughly 1/2 of the xylobiose had been consumed, yielding xylose and xylotriose in a ~4:1 ratio. Two peaks in the region corresponding to xylotriose were observed on the electropherogram, and it is not clear at this time if that is caused by different isomers of xylotriose being formed. While it appears that the enzyme was able to release xylose from both xylotriose and xylotetraose, the enzyme was inhibited by substrate concentrations greater than ~2 mM for either substrate. Substrate inhibition by xylotriose (K_i=1.7 mM) and no inhibition by xylobiose have previously been observed for a closely related *Thermoanaerobacterium* sp. GH family 39 β-D-xylosidase [8] and for an arabinofuranosidase isolated from a compost starter mixture[22]. The enzyme was not inhibited by up to 200 mM xylose, which is a potentially useful bioprocess characteristic. There is considerable variability in the susceptibility of xylosidases to product inhibition. For example, xylosidase from the fungus *Scytalidium thermophilum* was likewise not inhibited by up to 200 mM xylose [23], whereas a xylosidase from the thermophile *Caldocellum saccharolyticum* had a K_i for xylose of 40 mM [24].

Substrate Specificity

To assign the substrate specificity of BH1068(His)$_6$, a series of artificial and natural substrates were tested. Whereas it has previously been reported that BH1068(His)$_6$ is unable to cleave *p*-NP-AraF and weakly hydrolyzes *p*-NP-β-D-glucopyranoside [12], in this study BH1068(His)$_6$ was able to cleave the arabinofuranosyl, arabinopyranosyl, and xylopyranosyl synthetic aryl substrates, whereas no activity was detected with the other aryl-glycoside synthetic substrates tested. D-xylopyranose, L-arabinofuranose, and L-arabinopyranose are all spatially similar, thereby, rationalizing the multifunctional α-L-arabinofuranosidase/α-L-arabinopyranosidase/β-D-xylosidase activity of BH1068(His)$_6$ with respect to hydrolysis of synthetic substrates containing the relatively good leaving groups *o*-NP (p*K*a=7.22) or *p*-NP (p*K*a=7.18). In the natural substrate, however, the leaving groups are either xylose or arabinose moieties, which are very poor leaving groups with p*K*a>12. When hydrolysis of natural substrate glycosidic bonds by BH1068(His)$_6$ was tested, only release of xylose was observed by CE from rye, wheat, oat-spelt, beech, and birch arabinoxylan. Also, it was found that BH1068(His)$_6$ does not hydrolyze sugar beet arabinan containing (1–3)-α-linked L-arabinofuranosyl branch units. With respect to natural substrate specificity, it can, therefore, be concluded that BH1068(His)$_6$ is specific for hydrolyzing xylopyranosyl units.

pH Curve

Whereas alkaliphiles such as *B. halodurans* C-125 grow optimally at pH values above 9, the intracellular pH range is thought to be in the range between 7 and 8.5, and the pH optima of intracellular enzymes would be expected to be in this range [25]. A sharp pH optima was observed at pH 6.5 for BH1068(His)$_6$, in the same range as that found for several other xylanolytic activities isolated from this organism. Thus, two types of xylanase from *Bacillus halodurans* C-125 have been expressed in *E. coli*; xylanase N had a pH optima between 6 and 7, whereas xylanase A had a broad activity range from pH 6 to 10 [26]. A GH family 8 reducing-end xylose-releasing exooligoxylanase gene has also been expressed from this organism (*BH2105*) and was found to have a pH optimum of 6.2 to 7.3 [27]. Similar pH optima were also found for four xylanases isolated from thermophilic *Bacillus* strains; the optima for strains W1 and W3 was pH 6.0, and for strains W2 and W4, the optima were between pH 6 and 7 [28].

Thermal Stability and T_{max}

The enzyme was stable for 10 min up to 45°C, whereas the activity decreased rapidly to ~30% after 10 min at 55°C (Fig. 2). The temperature maximum (T_{max}) was found to be 47°C under the conditions tested (30 min endpoint assays), whereupon activity rapidly diminished, possibly because of enzyme thermal instability.

Acknowledgment The mention of firm names or trade products does not imply that they are endorsed or recommended by the US Department of Agriculture over other firms or similar products not mentioned. All programs and services of the US Department of Agriculture are offered on a non-discriminatory basis without regard to race, color, national origin, religion, sex, age, marital status, or handicap.

References

1. Bajpai, P. (1997). *Advances in Applied Microbiology, 43*, 141–195.
2. Rahman, A. K. M. S., Sugitani, N., Hatsu, M., & Takamizawa, K. (2003). *Canadian Journal of Microbiology, 49*, 58–64.
3. Sørensen, H. R., Pedersen, S., Viksø-Nielsen, A., & Meyer, A. S. (2005). *Enzyme and Microbial Technology, 36*, 773–784.
4. Saha, B. C. (2003). *Journal of Industrial Microbiology & Biotechnology, 30*, 279–291.
5. Biely, P. (2003). In J. R. Whitaker, A. G. J. Voragen, & D. W. S. Wong (Eds.) *Handbook of food enzymology* pp. 879–915. New York: Marcel Dekker.
6. Shallom, D., & Shoham, Y. (2003). *Current Opinion in Microbiology, 6*, 219–228.
7. Beg, Q. K., Kapoor, M., Mahajan, L., & Hoondal, G. S. (2001). *Applied Microbiology and Biotechnology, 56*, 326–338.
8. Wagschal, K., Franqui-Espiet, D., Lee, C. C., Robertson, G. H., & Wong, D. W. S. (2005). *Applied and Environmental Microbiology, 71*, 5318–5323.
9. Coutinho, P. M., & Henrissat, B. (1999). In H. J. Gilbert, D. Davies, B. Henrissat, & B. Svensson (Eds.) *Recent advances in carbohydrate bioengineering* pp. 3–12. Cambridge: The Royal Society of Chemistry.
10. Czjzek, M., David, A. B., Bravman, T., Shoham, G., Henrissat, B., & Shoham, Y. (2005). *Journal of Molecular Biology, 353*, 838–846.
11. Yang, J. K., Yoon, H. J., Ahn, H. J., Lee, B. I., Pedelacq, J. D., & Liong, E. C., et al. (2004). *Journal of Molecular Biology, 335*, 155–65.
12. Smaali, I., Rémond, C., & O'Donohue, M. J. (2006). *Applied Microbiology and Biotechnology, 73*, 582–590.
13. Davies, G., & Henrissat, B. (1995). *Structure, 3*, 853–859.
14. Gebler, J., Gilkes, N., Claeyssens, M., Wilson, D., Beguin, P., & Wakarchuk, W., et al. (1992). *Journal of Biological Chemistry, 267*, 12559–12561.
15. Koshland, D. E. (1953). *Biological Reviews, 28*, 416–436.
16. Zechel, D. L., & Withers, S. G. (2000). *Accounts of Chemical Research, 33*, 11–18.
17. Vocadlo, D. J., Wicki, J., Rupitz, K., & Withers, S. G. (2002). *Biochemistry, 41*, 9727–9735.
18. Ly, H. D., & Withers, S. G. (1999). *Annual Reviews of Biochemistry, 68*, 487–522.
19. Lee, Y.-E., & Zeikus, G. (1993). *Journal of General Microbiology, 139*, 1235–1243.
20. Bravman, T., Belakhov, V., Solomon, D., Shoham, G., Henrissat, B., Baasov, T., & Shoham, Y. (2003). *Journal of Biological Chemistry, 278*, 26742–26749.
21. Vocadlo, D. J., Wicki, J., Rupitz, K., & Withers, S. G. (2002). *Biochemistry, 41*, 9736–9746.
22. Wagschal, K., Franqui-Espiet, D., Lee, C. C., Kibblewhite-Accinelli, R. E., Robertson, G. H., & Wong, D. W. S. (2007). *Enzyme and Microbial Technology, 40*, 747–753.
23. Zanoelo, F. F., de Lourdes Teixeira de Moraes Polizeli, M., Terenzi, H. F., & Jorge, J. A. (2004). *Journal of Industrial Microbiology & Biotechnology, 31*, 170–176.
24. Hudson, R. C., Schofield, L. R., Coolbear, T., Daniel, R. M., & Morgan, H. W. (1990). *Biochemical Journal, 273*, 645–650.
25. Horikoshi, K. (2004). *Proceedings of the Japan Academy, Series B, 80*, 166–178.
26. Honda, H., Kudo, T., Ikura, Y., & Horikoshi, K. (1985). *Canadian Journal of Microbiology, 31*, 538–542.
27. Honda, Y., & Kitaoka, M. (2004). *Journal of Biological Chemistry, 279*, 55079–55103.
28. Okazaki, W., Akiba, T., Horikoshi, K., & Akahoshi, R. (1985). *Agricultural and Biological Chemistry, 49*, 2033–2039.